Journal of Biomechanics 48 (2015) 3718–3724

Contents lists available at ScienceDirect

Journal of Biomechanics

journal homepage: www.elsevier.com/locate/jbiomech
www.JBiomech.com

Apportionment of lumbar L2–S1 rotation across individual motion segments during a dynamic lifting task

Ameet Aiyangar [a], Liying Zheng [b], William Anderst [b], Xudong Zhang [b,c,d,*]

[a] EMPA, Swiss Federal Laboratories for Materials Science and Technology, Mechanical Systems Engineering, Ueberlandstrasse 129, 8400 Duebendorf, Switzerland
[b] Department of Orthopaedic Surgery, University of Pittsburgh, Pittsburgh, PA 15261, USA
[c] Department of Bioengineering, University of Pittsburgh, Pittsburgh, PA 15261, USA
[d] Department of Mechanical Engineering and Materials Science, University of Pittsburgh, Pittsburgh, PA 15261, USA

ARTICLE INFO

Article history:
Accepted 18 August 2015

Keywords:
Lumbar spine
Vertebral motion
Apportionment
Dynamic stereo X-ray
Lifting

ABSTRACT

Segmental apportionment of lumbar (L2–S1) rotation is a critical input parameter for musculoskeletal models and a candidate metric for clinical assessment of spinal health, but such data are sparse. This paper aims to quantify the time-variant and load-dependent characteristics of intervertebral contributions to L2–S1 extension during a dynamic lifting task. Eleven healthy participants lifted multiple weights (4.5, 9.1, and 13.6 kg) from a trunk-flexed to an upright position while being imaged by a dynamic stereo X-ray system at 30 frames/s. Vertebral (L2–S1) motion was tracked using a previously validated volumetric model-based tracking method that employs 3D bone models reconstructed from subject-specific CT images to obtain high-accuracy ($\leq 0.26°$, 0.2 mm) 3D vertebral kinematics. Individual intervertebral motions as percentages of the total L2–S1 extension were computed at each % increment of the motion to show the segmental apportionment. Results showed L3–L4 ($25.8 \pm 2.2\%$) and L4–L5 ($31 \pm 3.1\%$) together contributed a larger share (~60% combined) compared to L2–L3 ($21.7 \pm 3.7\%$) and L5–S1 ($22.6 \pm 4.7\%$); L4–L5 consistently provided the largest contribution of the measured segments. Relative changes over time in L3–L4 ($6 \pm 12.5\%$) and L4–L5 ($0.5 \pm 10.2\%$) contribution were minimal; in contrast, L2–L3 ($18 \pm 20.1\%$) contribution increased while L5–S1 ($-33 \pm 22.9\%$) contribution decreased in a somewhat complementary fashion as motion progressed. No significant effect of the magnitude of load lifted on individual segmental contribution patterns was detected. The current study updated the knowledge regarding apportionment of lumbar (L2–S1) motion among individual segments, serving both as input into musculoskeletal models and as potential biomechanical markers of low back disorders.

© 2015 Elsevier Ltd. All rights reserved.

1. Introduction

A clear understanding of lumbar biomechanics has implications on both the treatment and prevention of low back disorders (LBD). From a clinical perspective, treatment of chronic LBD aims to restore normal functional motion, in addition to the more subjective goal of mitigating pain symptoms. From a prevention perspective, recognition and control of biomechanical risk factors require a thorough understanding of force and stress distributions within the spine during functional tasks. In both cases, an accurate description of dynamic, three-dimensional (3D) vertebral kinematics is necessary (Waters et al., 1993). This is because (a) normal functional motion benchmarks are mainly based on kinematic measures, and (b) given the infeasibility of direct measurement, *in vivo forces* experienced by lumbar tissue structures are estimated from biomechanical models (Cholewicki et al., 1991; de Zee et al., 2007; Han et al., 2012; Senteler et al., 2015; Stokes and Gardner-Morse, 1995; Waters et al., 1993; Zhu et al., 2013), the process of which is highly sensitive to the quality of kinematic input.

Segmental range of (rotational) motion (ROM) determined from static, lateral radiographs of end-range flexion–extension positions has traditionally been the primary kinematic parameter used in clinical diagnoses—although its efficacy in distinguishing between patients with disorders and asymptomatic ones has been questioned (Ellingson et al., 2013; Lehman, 2004)—and in assessing the success of treatment procedures, particularly those requiring surgical intervention. While ROM is an important, yet simple metric for assessing lumbar joint function, it is, by itself, inadequate for characterizing lumbar motion. For example, the contribution to overall lumbar rotation may differ between individual segments (Ahmadi et al., 2009; Panjabi et al., 1994; Pearcy et al., 1984; Wong et al., 2004) and, more importantly, ROM-based kinematic evaluations may not appropriately

* Corresponding author at: Department of Mechanical Engineering and Materials Science, 636 Benedum Hall, University of Pittsburgh, Pittsburgh, PA 15261, USA. Tel.: +1 412 624 5430; fax: +1 412 624 7661.
E-mail address: xuz9@pitt.edu (X. Zhang).

http://dx.doi.org/10.1016/j.jbiomech.2015.08.022
0021-9290/© 2015 Elsevier Ltd. All rights reserved.

represent differences in mid-range rotational characteristics (Anderst et al., 2008; Teyhen et al., 2007) between healthy and pathologically- or surgically-altered spines. Secondly, accurate data regarding the apportionment of lumbar rotation, particularly during functional, daily living activities, are a critical input for musculoskeletal biomechanical models. Musculoskeletal models (Christophy et al., 2012; de Zee et al., 2007; Han et al., 2012; Senteler et al., 2014) often define segmental kinematics based on constant fractions of overall lumbar motion. Given this context, quantifying the apportionment of lumbar rotation across its individual segments and clarifying its time-variant and load-dependent characteristics could have a direct positive impact on the accuracy of model predictions, while also potentially leading to improved biomechanical markers of pathological conditions.

Several studies have attempted to quantify segmental contributions to overall lumbar rotation. These include *in vitro* cadaveric studies (Goel et al., 1985; Miller et al., 1986; Schultz et al., 1979; Soni et al., 1982; Tencer et al., 1982), *in vivo* studies based on 2D lateral radiographs or static biplane radiography (Li et al., 2009; Passias et al., 2011; Pearcy et al., 1984; Plamondon et al., 1988), surface marker-based studies (Troke et al., 2001; Zhang and Xiong, 2003), uniplanar continuous radiography (Ahmadi et al., 2009; Harada et al., 2000; Kanayama et al., 1995; Okawa et al., 1998; Wong et al., 2004; Wong et al., 2006), and, more recently, dynamic biplane radiography (Aiyangar et al., 2014; Anderst et al., 2008; Wu et al., 2014). These studies have collectively and progressively improved our understanding of lumbar spinal motion. However, reported results regarding segmental contribution patterns have been inconsistent. Some studies have reported an increased contribution from caudal segments (L4–5, L5–S1) compared to the cephalic segments (Panjabi et al., 1994; Pearcy et al., 1984), others have reported a progressively decreasing contribution from cephalic to caudal segments (Li et al., 2009; Wong et al., 2004; Wong et al., 2006), while still others failed to detect significant differences in contributions (Aiyangar et al., 2014; Goel et al., 1985; Schultz et al., 1979; Tencer et al., 1982; Wu et al., 2014). Differences in experimental protocols do not completely account for these variations as the inconsistency persists even between studies using similar techniques. For example, while Pearcy et al. (1984) and Plamondon et al. (1988) reported an increased contribution from caudal segments compared to cephalic segments from their static biplane X-ray imaging studies, Li et al. (2009) observed the opposite using comparable methods. Harada et al. (2000), using continuous X-ray imaging studies where the pelvis was restrained, reported a phase lag between segments while Wu et al. (2014) and Teyhen et al. (2005) reported simultaneous contributions. Comparing studies that eschewed explicit pelvic restraints, Wong et al. (2004) reported a progressively decreasing contribution from L1–2 to L5–S1, but these results were not replicated in a study by Ahmadi et al. (2009). As a result, how total lumbar rotation is apportioned across its individual segments throughout a movement remains unresolved.

Therefore, the purpose of the current study was to map the continuous segmental percent contributions to lumbar extension motion during load lifting—a common functional activity— and seek answers to the following questions: (1) Do some segments bear a larger share of lumbar rotation compared to others? (2) Does this contribution remain constant over the entire range of motion, or does it vary from beginning to end? (3) Does the amount of external load borne during a particular task affect the distribution of lumbar rotation across its segments?

Note: Due to limitations in the dimensions of the experimental setup, only vertebrae from L2–S1 were observed in this study. Hence readers are informed that the term “lumbar” henceforth refers only to “L2–S1” and does not include T12–L1 and L1–L2 joint information.

2. Methods

With institutional review board (IRB) approval, 14 healthy participants (eight male, six female) between the ages of 19 and 30, and a waist size no greater than 89 cm (35 in.) (Table 1) were recruited for the study. Participants reported no prior history of LBD. The quantified risks of the study including radiation exposure were explained to each participant, and each participant read and signed an IRB-approved informed consent document prior to participating in the study. Participants' lumbar regions were imaged by a dynamic stereo X-ray (DSX) system while they performed multiple lifting trials. The details regarding the lifting protocol, apparatus, imaging and data acquisition techniques have been delineated in a previous publication (Aiyangar et al., 2014). What follows is a brief summary along with additional details regarding aspects of the current study not already covered in the previous publication.

2.1. Lifting task

Starting from a trunk-flexed (~75° flexion) position, participants lifted an object of known weight (three weight levels: 4.5 kg, 9.1 kg and 13.6 kg) up to a final, upright position in a sagittally symmetric manner. The object was positioned at an approximate height of 35 cm from the floor and about 30 cm away horizontally from the upright body position. Minor adjustments on account of differences in participant's height were made to the positioning of the object in order to control for the amount of sagittal trunk ROM (~75° flexion), while simultaneously ensuring, based on participants' own feedback, that the starting position posed no discomfort due to excessive flexion. Handles were affixed onto the weight-bearing dowel perpendicular to its length and approximately shoulder width apart (38 cm). The initial flexed position was determined with a goniometer, as the angle made at the hip by surface markers placed at the shoulder and knee. Participants were instructed to complete the lift primarily with trunk extension without knee bending (*i.e.* a back- or stoop-lift strategy). Two trials were performed per weight level, each taking two seconds or less, resulting in a maximum of six trials per participant. The tasks were not randomized; rather the weight levels were increased progressively from lowest to the highest. Adequate rest was provided between each trial, as requested by the participants.

2.2. Data acquisition

The DSX system simultaneously recorded dynamic X-ray images of the participants' lumbar spines in medial–lateral (ML) and anterior–posterior (AP) directions as they performed lifting tasks (60 frames at 30 fps, pulsed exposure time = 4 ms/frame, excitation voltage = 70–80 kV, current = 320–630 mA). Back-and-forth pelvic motion in the sagittal plane was partially limited (but not completely eliminated) by instructing participants to maintain light but constant contact between their pelves and a semi-rigidly constructed *Pelvic Rest*.[1] A few practice lifts were sufficient to train the participants to adhere to this condition and no additional external feedback mechanism was required. Barring the constraint of having to maintain contact with the Pelvic Rest throughout the motion, the pelvis was otherwise unrestrained. A custom-built *radiation attenuator* was used to minimize radiation whiteout effects (Aiyangar et al., 2014). Following testing, high resolution computed tomography (CT) scans (voxel size = 0.25 mm × 0.25 mm × 1.25 mm) of the participants' lumbar spines were obtained (GE Light Speed Pro 16, GE Medical Systems, Waukesha, WI). Individual vertebrae were segmented to create 3D bone models using Mimics 14.0 (Materialise Inc., Ann Arbor, MI). The effective radiation dose from DSX recording of all the trials, determined using PCXMC simulation software (STUK, Helsinki, Finland), was less than 3.6 mSv, while the maximum estimated effective radiation dose from CT was less than 12.33 mSv.

2.3. Model-based tracking

A previously validated model-based tracking process was used to determine instantaneous 3D vertebral position with sub-millimeter accuracy [precision $\leq 0.26°$, 0.2 mm (Lee and Anderst, 2010)]. Detailed descriptions have been extensively published elsewhere (Aiyangar et al., 2014; Anderst et al., 2008; Lee and Anderst, 2010). Briefly, a virtual DSX system proportionally and configurationally identical to the experimental setup generates digitally reconstructed radiographs (DRR) of the 3D CT-derived model of a vertebra. The DRRs are registered to the experimental DSX images *via* a ray-tracing algorithm in an iterative process that is largely automatic, with some manual refining. The correlation is maximized using a volumetric image-matching algorithm to determine, frame-wise, the 3D pose of the vertebra. Repeating this process separately for

[1] Limiting backward pelvic motion while bending forward from an erect position could result in a tendency to fall forward. In order to avoid this, participants were asked to position themselves for the task with their feet slightly forward. Participants were then encouraged to align their feet as closely with the hips as possible in the sagittal plane without feeling they would fall over if they bent forward. Hence participants were almost, but not completely erect when they attained the final “upright” position at the end of the lifting task.

Table 1
Participants' anthropometric and age information presented as mean ± SD values.

Volunteers	Height (cm)	Weight (kg)	Waist size (cm)	Age (years)
Male	178 ± 7	78 ± 9	83 ± 5	24 ± 2
Female	170 ± 6	61 ± 8	73 ± 9	25 ± 2
All	175 ± 8	71 ± 12	79 ± 8	24 ± 2

each vertebra across 60 frames of data, the software then outputs 3D kinematics (three rotations and three translations) of each bone.

2.4. Kinematic analysis

Anatomical coordinate systems (ACS) (Wu et al., 2002) were defined for each vertebra by three mutually orthogonal axes—AP, ML, and superior–inferior (SI)—with the origin at the center of the vertebral body, located as the average of eight digital markers placed on the vertebral body of the bone models. Ordered body-fixed rotations and translations were extracted from homogenous transformation matrices for each segment (L2–L3, L3–L4, L4–L5, and L5–S1) by relating frame-by-frame position of the superior vertebral ACS relative to the inferior vertebral ACS. In order to standardize representation of motion across participants, the starting, flexed overall lumbar (L2–S1 in this study) pose assumed for the lifting task was defined as 0%, while the static upright position of each participant was taken as reference and defined as 100%. L2–S1 pose in the final recorded frame, *i.e.* at the end of the lifting task, however, may not have matched the static upright L2–S1 pose. Hence, the normalized kinematics were further corrected by multiplying the data with a weighting factor representing the fraction of the "ideal" achievable amount of L2–S1 extension reached by participant during the task, assuming the "ideal", at 100%, was the static upright position. This step standardized the *abscissa* for all study participants (0–100% of L2–S1 ROM). Rotation angles were then interpolated to obtain segmental rotations for each percentage point increment of the L2–S1 ROM. Percent segmental contribution to the instantaneous lumbar (L2–S1) extension was then computed at every percentage point increment of L2–S1 ROM.

2.5. Statistical analysis

Data from the initial few frames (< 10% ROM) exhibited a much larger scatter than in subsequent frames. Initial segmental angular displacements are small (< 0.5°) and close to the precision limit of the DSX system. Since we are reporting relative contributions, even relatively small absolute errors introduce large relative errors (*e.g.* 0.5° error = 100% relative error) beyond any inherent intra- and inter-subject variability and exert an undue influence on the aggregated datasets. Secondly, participants' L2–S1 extension exceeded 90% of their upright static posture only in about half the trials and most reached between 80% and 90% before ending the lift. Hence, only data between 10% and 80% of total L2–S1 ROM has been included in the following analysis.

Where two trials were successfully recorded per lifting task, they were averaged into a single dataset to represent each participant's motion for that particular task. Mean (μ) and ± 95% confidence interval (CI_{95}) values across all participants were computed at each percent increment of the L2–S1 ROM for each weight lifting task.

Data across the three weight lifting tasks were then aggregated (collapsed across task level) to present an averaged pattern of instantaneous segmental contribution. Finally, the percent-wise data were further aggregated (collapsed across time) into a single value ($\bar{x} \pm CI_{95}$) representing the motion-wide average contribution for each segment. Statistical significance regarding the differences between segments could be visually inspected based on the extent of overlap between the $\pm CI_{95}$ bands: no overlap indicates differences in means are statistically significant.

3. Results

Data from three participants had substantial portions that were non-trackable due to poor image quality and therefore were excluded. Results from the remaining 11 participants (seven male, four female) are organized according to the questions raised as follows.

Do some segments bear a larger share of lumbar rotation compared to others?

The ensemble dataset—continuous data collapsed across weights lifted and time (Fig. 1)—showed the inner segments (L3–L4: $\bar{x} \pm CI_{95} = 25.8 \pm 2.2\%$; L4–L5: $\bar{x} \pm CI_{95} = 31.0 \pm 3.1\%$) together contributing a larger share of L2–S1 motion compared to L2–L3 ($\bar{x} \pm CI_{95} = 21.7 \pm 3.7\%$) and L5–S1 ($\bar{x} \pm CI_{95} = 22.6 \pm 4.7\%$). L4–L5 was the largest contributor and was significantly greater than L2–L3 and L5–S1. L2–L3 and L5–S1 contributions were the smallest of the four segments studied and appeared comparable on average. Segmental extension ROMs observed in this study are presented in Table 2.

Does individual segmental contribution remain constant over the entire range of motion, or does it vary from beginning to end?

Continuous curves of the uncollapsed data (Fig. 2a–c) delineate the mean relative segmental contributions at each of the three weight levels, 4.5, 9.1 and 13.6 kg respectively (color-coded bands represent $\pm CI_{95}$), while the collapsed data show the contributions combining the three weight levels (Fig. 2d). The same plots can be re-arranged comparing the three weight levels in order to visually clarify the influence of weight lifted on each intervertebral segment separately (Fig. 3).

Weight-specific data curves showed a pattern generally similar to the ensemble data, but with some subtle deviations. While L4–L5 contribution was consistently the largest across the weight levels, it was not always significantly greater than L5–S1 contributions throughout the motion. Complete separation of L4–L5 and L5–S1 CI_{95} regions was only seen beyond 40% of the overall L2–S1 motion (Fig. 2). L2–L3 contribution, however, appeared significantly lower than L4–L5 throughout the motion except for the highest weight task, where non-overlapping CI_{95} regions only occurred beyond the 50% L2–S1 ROM mark. Contributions from L3–L4 and L4–L5, on average, remained largely unchanged during the motion (Figs. 2d, 3b and c, and 4). L5–S1 contribution exhibited a gradual decrease ($-33.1 \pm 22.9\%$) as motion progressed (Figs. 2d, 3d, and 4), which was consistent across weight levels. Except for the highest weight level, L2–L3 contribution increased ($18.0 \pm 20.8\%$) in a somewhat complementary fashion (Figs. 2d, 3a, and 4).

Does the amount of external weight borne during a particular task affect the distribution of lumbar rotation across its segments?

No significant effect of the magnitude of load lifted on the relative contribution of each segment was detected. The curves representing the mean contributions at any given weight level were encompassed within the $\pm CI_{95}$ bands of the other two levels for the observed segments (Fig. 3).

4. Discussion

Past studies, largely, have not delved sufficiently into the potential time and load dependency of individual segmental rotation. The aim of the current study was to gain insight into how dynamic lumbar rotation during functional motion is shared across the individual segments and, more importantly, note the sensitivity of this apportionment to the variation in external loading. A sagittally symmetric lifting task was well suited to answer this question as it is considered a common daily living activity or occupational task, which is also purportedly associated with the risk of low back disorders.

Inner segments contributed a larger amount, with smaller contributions from segments at both the cephalic and caudal ends. Ahmadi et al.'s (2009) study appears to be the only other study in the literature that has reported agreeable results. Although relative segmental contributions were not directly discussed in that study, by computing the relative segmental contributions from the reported relevant segmental ranges of motion, we obtained percentages (approximately 18%, 25%, 32% and 25% for L2–L3, L3–L4, L4–L5 and L5–S1 respectively), and thus a contribution pattern, which was in general agreement with the current study results.

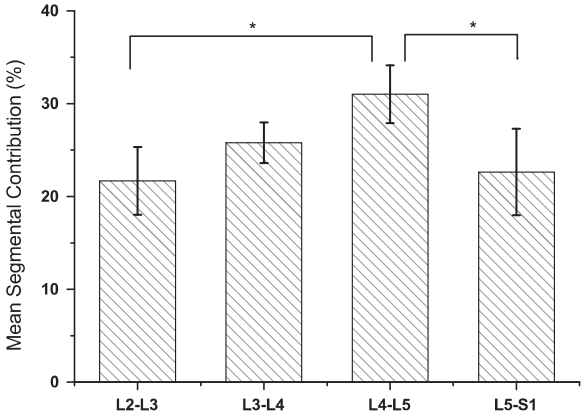

Fig. 1. Mean segmental contributions to total L2–S1 extension obtained by collapsing the continuous datasets across time and over the three load lifting trials. Errors bars represent ±95% confidence intervals. [*] indicates significant differences based on non-overlapping error bars.

Table 2
Maximum intervertebral extensions during the lifting task.

Intervertebral segment	Extension range of motion (deg)	
	Mean	95% CI
L2–L3	9.9	1.5
L3–L4	10.7	1.4
L4–L5	12.1	2.0
L5–S1	9.6	2.1
L2–S1	43.6	4.4

Recently published preliminary results by our group (Aiyangar et al., 2014) reported a lack of significant differences between the segmental contributions, although a consistently smaller contribution from L5–S1 was noted. Those results were based on a smaller subset—a single trial of the lowest weight lifting task (4.5 kg) of six male participants. The current, full dataset included almost twice the number of participants, with a majority of participants completing two trials for each task (52 trials, 30 motion datasets). The larger sample size appears to have sufficiently improved the ability to discern some differences in the individual segmental contributions, which could, at best, only be noticed as a weak trend in the previous study. On the other hand, any apparent incongruity between the results from the preliminary and full datasets also points to the high inter-subject variability present within the continuous contribution curves.

Since changes occurring within the lumber segments during motion seem modest, the aggregated, ensemble dataset (Fig. 2) appears to represent the overall apportionment of motion across the individual segments reasonably well. However, looking at only the aggregated dataset masks the subtler changes in the contribution of – and possible interaction between – L5–S1 and L2–L3 joints. Secondly, L5–S1 contribution was much larger at the more markedly flexed positions of the flexion-to-upright lumbar ROM [~75° gross initial trunk flexion; corresponding initial L2–S1 flexion ($\bar{x} \pm CI_{95}$) = 44 ± 4°], with somewhat correspondingly smaller L2–L3 contribution. Changes in relative segmental contributions were only observed within the first half of the lumbar ROM. While the changing pattern of segmental contributions over the motion seen in this study would definitely get missed in static end-range ROM evaluations, it is plausible that this feature might also go undetected in investigations of less extensive lumbar ROMs. The larger contribution from L5–S1 near full flexion

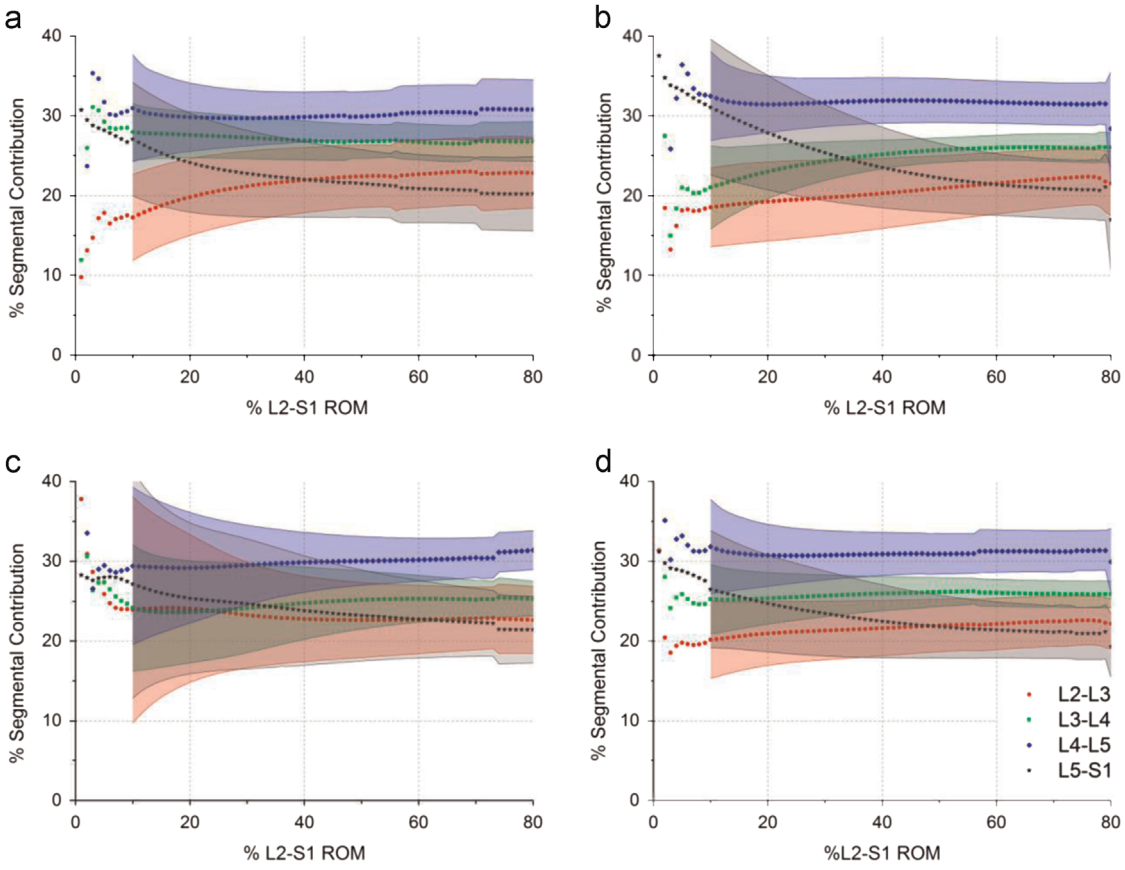

Fig. 2. Apportionment of L2–S1 extension across individual segments shown for each weigh level: (a) 4.5 kg, (b) 9.1 kg, (c) 13.6 kg, and (d) mean across all three weight levels. Due to large scatter in data from the first few frames CI_{95} bands for initial 10% L2–S1 ROM have not been included.

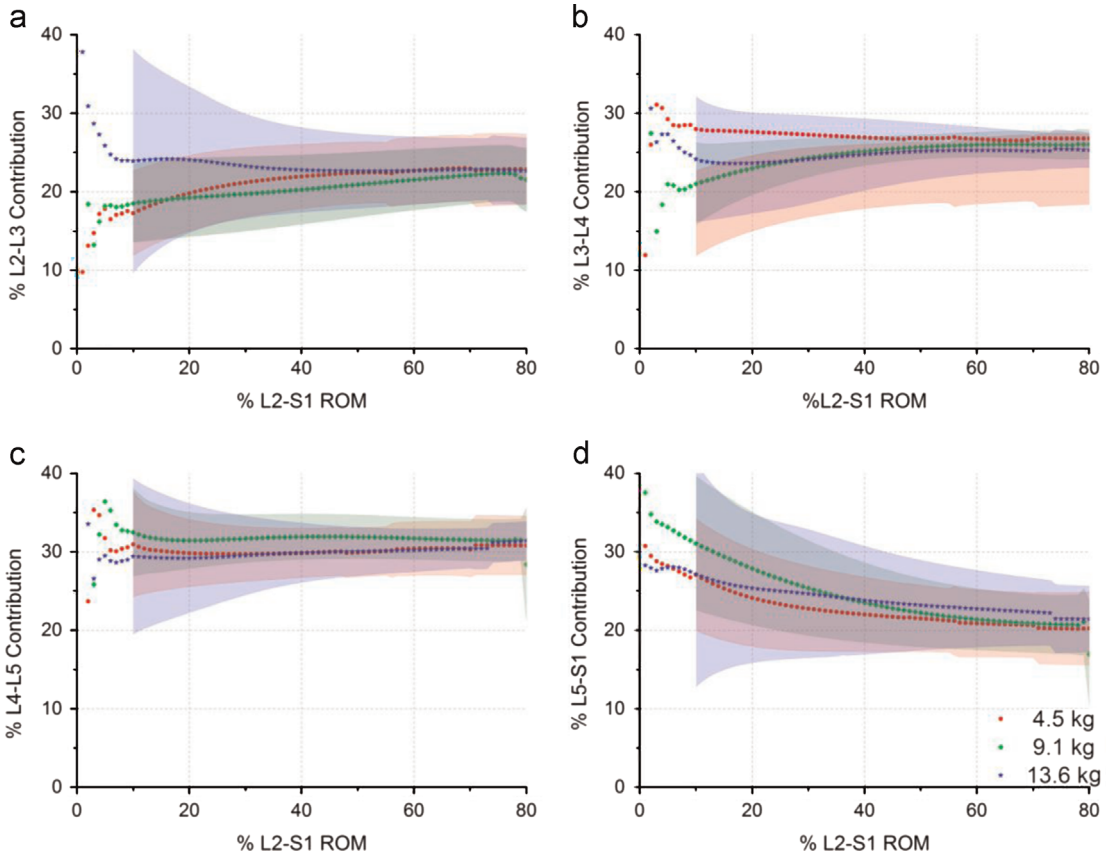

Fig. 3. Effect of load lifted on segmental contribution to L2–S1 extension. Color-coded bands represent ±95% confidence intervals. (a) L2–L3, (b) L3–L4, (c) L4–L5, and (d) L5–S1. Due to large scatter in data from the first few frames CI_{95} bands for initial 10% L2–S1 ROM have not been included.

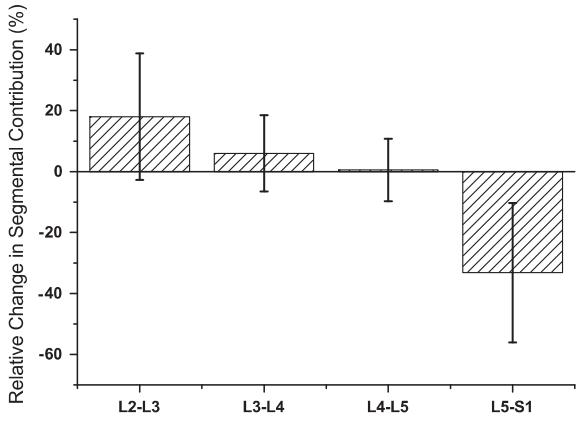

Fig. 4. Relative change over time in the percent contribution (100*(final − initial)/final) from each segment to total L2–S1 extension over the entire lifting motion. Error bars are ±95% confidence intervals.

appears to be in agreement with a recent study on lumbo-pelvic rhythm (Tafazzol et al., 2014), which showed a dominant contribution from the pelvis during the initial stages of lumbo-pelvic extension motion, with the lumbar region's contribution catching up towards the end. Alternatively, Harada et al. (2000) reported a phase lag between segmental contributions wherein initial contribution begins at L5–S1 with subsequent involvement of the upper segments progressively. Lee et al. (2002), however, have suggested that this "phase lag" could actually have been an inability to measure the smaller initial rotations in L3–L4 and L4–L5 compared to L5–S1, implying that Harada et al.'s results should be interpreted as simultaneously occurring motion with larger contributions from L5–S1 at the beginning of an extension motion. If true, this would further imply that, deploying a pelvic restraint, as done by Harada et al. and others (Okawa et al., 1998; Teyhen et al., 2007; Wu et al., 2014), *might not significantly* alter lumbar motion profiles, although it obviously precludes an accounting of the pelvic contribution, which, as Tafazzol et al. have shown, can be significant. The flexed spine also experiences the largest compressive forces compared to other postures (Anderson et al., 1986; Han et al., 2012; Schultz et al., 1982; Senteler et al., 2015; Tafazzol et al., 2014; Wilke et al., 1999). Overloading has particularly been shown to be a prominent biomechanical risk factor for L5–S1 disk disorders (Waters et al., 1993). The unique segment-wise motion distribution patterns seen in the flexed positions are, then, likely a way to optimize spinal loading, particularly at the L5–S1 level, as suggested by Tafazzol et al. (2014).

Overall, the magnitude of weight lifted had a negligible effect on the distribution of lumbar rotation across its segments. Some past studies evaluating the effect of static external loads on lumbosacral vertebral orientation found no significant effect of the load lifted on vertebral orientation (Anderson et al., 1986; Lee and Chen, 2000). They rationalized that the moment generated by the upper body weight dominated those generated by the external loads. Lee and Chen (2000), however, further found that a lordotic posture generated a stronger effect of external load compared to a kyphotic posture. Since the lifting technique employed in this study was essentially a stoop lift, participants' lumbar spines were predominantly in a kyphotic posture. While the lack of significant influence from external loading on the segmental apportionment of lumbar extension appears to be consistent with the static studies mentioned above, we plan to specifically investigate this topic in the near future by incorporating these newly acquired kinematics into a rigid body musculoskeletal lumbar spine model.

We acknowledge the following limitations of the study. First, we only included participants less than 30 years of age and waist size no greater than 89 cm (35 in.) with a self-reported healthy status of the spine, thereby potentially limiting broad applicability of the conclusions. Second, although both male and female participants were included in this study, sex differences were not explicitly assessed, due to the fact that sample sizes were deemed too small to obtain reasonable confidence in conclusions. This, however, does not necessarily imply equivalent rotational patterns between sexes. Third, while our data covered a fairly large range of movement, total ROM (*i.e.* approaching flexibility limits) was not evaluated. Consequently, we cannot conclusively state how contributions would be affected at extreme flexion positions. Finally, we did not assess spinal motion and the effects of external loading during a forward flexion motion. Results from some past *in vivo* studies (Ahmadi et al., 2009; Harada et al., 2000; Tafazzol et al., 2014) seem to imply that sagittal motion profiles are possibly path independent and joints might assume similar poses at the same "instant" of ROM during flexion and extension. Nevertheless, not explicitly recording motion during forward flexion, in addition to extension, limits the ability to generalize or extrapolate the kinematic data gathered to model the forward flexion movement of the spine, particularly with respect to understanding the effect of external loading.

Conflicts of interest statement

The authors have no conflict of interest related to the manuscript or the work it describes.

Acknowledgments

The work was funded by a research grant (R21OH00996) from the Centers for Disease Control and Prevention/National Institute for Occupational Safety and Health (CDC/NIOSH). Additional support was received through the Marie Sklowdoska-Curie Cofund Postdoctoral Fellowship Award. The authors thank Dr. Scott Tashman for technical advice on DSX data acquisition. The authors also thank Robert Carey for assistance with conducting the tests and Jonathan Foster, Michelle Schafman, George Kontogiannis, and Eric Ruth for assistance with data processing.

References

Ahmadi, A., Maroufi, N., Behtash, H., Zekavat, H., Parnianpour, M., 2009. Kinematic analysis of dynamic lumbar motion in patients with lumbar segmental instability using digital videofluoroscopy. Eur. Spine J. 18, 1677–1685.
Aiyangar, A.K., Zheng, L.Y., Tashman, S., Anderst, W.J., Zhang, X., 2014. Capturing three-dimensional in vivo lumbar intervertebral joint kinematics using dynamic stereo-X-ray imaging. J. Biomech. Eng. 136, 011004.
Anderson, C.K., Chaffin, D.B., Herrin, G.D., 1986. A study of lumbosacral orientation under varied static loads. Spine 11, 456–462.
Anderst, W.J., Vaidya, R., Tashman, S., 2008. A technique to measure three-dimensional in vivo rotation of fused and adjacent lumbar vertebrae. Spine J. 8, 991–997.
Cholewicki, J., McGill, S.M., Norman, R.W., 1991. Lumbar spine loads during the lifting of extremely heavy weights. Med. Sci. Sports Exerc. 23, 1179–1186.
Christophy, M., Faruk Senan, N.A., Lotz, J.C., O'Reilly, O.M., 2012. A musculoskeletal model for the lumbar spine. Biomech. Model. Mechanobiol. 11, 19–34.
de Zee, M., Hansen, L., Wong, C., Rasmussen, J., Simonsen, E.B., 2007. A generic detailed rigid-body lumbar spine model. J. Biomech. 40, 1219–1227.
Ellingson, A.M., Mehta, H., Polly, D.W., Ellermann, J., Nuckley, D.J., 2013. Disc degeneration assessed by quantitative T2* (T2 star) correlated with functional lumbar mechanics. Spine 38, E1533–E1540.
Goel, V.K., Goyal, S., Clark, C., Nishiyama, K., Nye, T., 1985. Kinematics of the whole lumbar spine. Effect of discectomy. Spine 10, 543–554.
Han, K.S., Zander, T., Taylor, W.R., Rohlmann, A., 2012. An enhanced and validated generic thoraco-lumbar spine model for prediction of muscle forces. Med. Eng. Phys. 34, 709–716.
Harada, M., Abumi, K., Ito, M., Kaneda, K., 2000. Cineradiographic motion analysis of normal lumbar spine during forward and backward flexion. Spine 25, 1932–1937.
Kanayama, M., Tadano, S., Kaneda, K., Ukai, T., Abumi, K., Ito, M., 1995. A cineradiographic study on the lumbar disc deformation during flexion and extension of the trunk. Clin. Biomech. 10, 193–199.
Lee J.B.E., Anderst W.J., 2010. Lumbar spine motion during functional movement: in vivo validation of flexion/extension movement tracking, In: Proceedings of 3rd Annual Lumbar Spine Research Society Meeting, Chicago, IL, USA.
Lee, S.W., Wong, K.W., Chan, M.K., Yeung, H.M., Chiu, J.L., Leong, J.C., 2002. Development and validation of a new technique for assessing lumbar spine motion. Spine 27, E215–E220.
Lee, Y.H., Chen, Y.L., 2000. Regressionally determined vertebral inclination angles of the lumbar spine in static lifts. Clin. Biomech. 15, 672–677.
Lehman, G.J., 2004. Biomechanical assessments of lumbar spinal function. How low back pain sufferers differ from normals. Implications for outcome measures research. Part I: Kinematic assessments of lumbar function. J. Manip. Physiol. Ther. 27, 57–62.
Li, G.A., Wang, S.B., Passias, P., Xia, Q., Li, G., Wood, K., 2009. Segmental in vivo vertebral motion during functional human lumbar spine activities. Eur. Spine J. 18, 1013–1021.
Miller, J.A., Schultz, A.B., Warwick, D.N., Spencer, D.L., 1986. Mechanical properties of lumbar spine motion segments under large loads. J. Biomech. 19, 79–84.
Okawa, A., Shinomiya, K., Komori, H., Muneta, T., Arai, Y., Nakai, O., 1998. Dynamic motion study of the whole lumbar spine by videofluoroscopy. Spine 23, 1743–1749.
Panjabi, M.M., Oxland, T.R., Yamamoto, I., Crisco, J.J., 1994. Mechanical behavior of the human lumbar and lumbosacral spine as shown by three-dimensional load-displacement curves. J. Bone Jt. Surg. Am. 76, 413–424.
Passias, P.G., Wang, S.B., Kozanek, M., Xia, Q., Li, W.S., Grottkau, B., Wood, K.B., Li, G. A., 2011. Segmental lumbar rotation in patients with discogenic low back pain during functional weight-bearing activities. J. Bone Jt. Surg. Am. 93A, 29–37.
Pearcy, M., Portek, I., Shepherd, J., 1984. Three-dimensional x-ray analysis of normal movement in the lumbar spine. Spine 9, 294–297.
Plamondon, A., Gagnon, M., Maurais, G., 1988. Application of a stereoradiographic method for the study of intervertebral motion. Spine 13, 1027–1032.
Schultz, A., Andersson, G., Ortengren, R., Haderspeck, K., Nachemson, A., 1982. Loads on the lumbar spine. Validation of a biomechanical analysis by measurements of intradiscal pressures and myoelectric signals. J Bone Jt. Surg. Am. 64, 713–720.
Schultz, A.B., Warwick, D.N., Berkson, M.H., Nachemson, A.L., 1979. Mechanical-properties of human lumbar spine motion segments. 1. Responses in flexion, extension, lateral bending, and torsion. J. Biomech. Eng. 101, 46–52.
Senteler, M., Weisse, B., Rothenfluh, D.A., Snedeker, J.G., 2015. Intervertebral reaction force prediction using an enhanced assembly of OpenSim models. Comput. Methods Biomech. Biomed. Eng., 1–11.
Senteler, M., Weisse, B., Snedeker, J.G., Rothenfluh, D.A., 2014. Pelvic incidence-lumbar lordosis mismatch results in increased segmental joint loads in the unfused and fused lumbar spine. Eur. Spine J. 23, 1384–1393.
Soni, A.H., Sullivan Jr., J.A., Patwardhan, A.G., Gudavalli, M.R., Chitwood, J., 1982. Kinematic analysis and simulation of vertebral motion under static load—Part I: Kinematic analysis. J. Biomech. Eng. 104, 105–111.
Stokes, I.A., Gardner-Morse, M., 1995. Lumbar spine maximum efforts and muscle recruitment patterns predicted by a model with multijoint muscles and joints with stiffness. J. Biomech. 28, 173–186.
Tafazzol, A., Arjmand, N., Shirazi-Adl, A., Parnianpour, M., 2014. Lumbopelvic rhythm during forward and backward sagittal trunk rotations: combined in vivo measurement with inertial tracking device and biomechanical modeling. Clin. Biomech. 29, 7–13.
Tencer, A.F., Ahmed, A.M., Burke, D.L., 1982. Some static mechanical properties of the lumbar intervertebral joint, intact and injured. J. Biomech. Eng. 104, 193–201.
Teyhen, D.S., Flynn, T.W., Bovik, A.C., Abraham, L.D., 2005. A new technique for digital fluoroscopic video assessment of sagittal plane lumbar spine motion. Spine 30, E406–E413.
Teyhen, D.S., Flynn, T.W., Childs, J.D., Kuklo, T.R., Rosner, M.K., Polly, D.W., Abraham, L.D., 2007. Fluoroscopic video to identify aberrant lumbar motion. Spine 32, E220–E229.
Troke, M., Moore, A.P., Maillardet, F.J., Hough, A., Cheek, E., 2001. A new, comprehensive normative database of lumbar spine ranges of motion. Clin. Rehabil. 15, 371–379.
Waters, T.R., Putz-Anderson, V., Garg, A., Fine, L.J., 1993. Revised NIOSH equation for the design and evaluation of manual lifting tasks. Ergonomics 36, 749–776.
Wilke, H.J., Neef, P., Caimi, M., Hoogland, T., Claes, L.E., 1999. New in vivo measurements of pressures in the intervertebral disc in daily life. Spine 24, 755–762.
Wong, K.W., Leong, J.C., Chan, M.K., Luk, K.D., Lu, W.W., 2004. The flexion–extension profile of lumbar spine in 100 healthy volunteers. Spine 29, 1636–1641.
Wong, K.W., Luk, K.D., Leong, J.C., Wong, S.F., Wong, K.K., 2006. Continuous dynamic spinal motion analysis. Spine 31, 414–419.
Wu, G., Siegler, S., Allard, P., Kirtley, C., Leardini, A., Rosenbaum, D., Whittle, M., D'Lima, D.D., Cristofolini, L., Witte, H., Schmid, O., Stokes, I., Standardization, Terminology Committee of the International Society of Biomechanics, 2002. ISB

recommendation on definitions of joint coordinate system of various joints for the reporting of human joint motion—Part I: Ankle, hip, and spine. International society of biomechanics. J. Biomech. 35, 543–548.
Wu, M., Wang, S., Driscoll, S.J., Cha, T.D., Wood, K.B., Li, G., 2014. Dynamic motion characteristics of the lower lumbar spine: implication to lumbar pathology and surgical treatment. Eur. Spine J. 23, 2350–2358.
Zhang, X., Xiong, J., 2003. Model-guided derivation of lumbar vertebral kinematics in vivo reveals the difference between external marker-defined and internal segmental rotations. J. Biomech. 36, 9–17.
Zhu, R., Zander, T., Dreischarf, M., Duda, G.N., Rohlmann, A., Schmidt, H., 2013. Considerations when loading spinal finite element models with predicted muscle forces from inverse static analyses. J. Biomech. 46, 1376–1378.

Reproduced with permission of the copyright owner. Further reproduction prohibited without permission.